Hindawi
Journal of Robotics
Volume 2018, Article ID 2914871, 7 pages
https://doi.org/10.1155/2018/2914871

Research Article

An Alignment Method of Human-Robot Collaboration Based on the Six-Dimensional Force/Torque Dynamic Measurement for Large-Scale Components

Ke Wen,[1] **Fuzhou Du**,[2] **Jiabo Zhang**,[1] **and JiZhi Yang**[1]

[1]*Beijing Spacecrafts, China Academy of Space Technology, Beijing 100194, China*
[2]*School of Mechanical Engineering and Automation, Beihang University, Beijing 100191, China*

Correspondence should be addressed to Fuzhou Du; du_fuzhou@163.com

Received 22 May 2018; Revised 23 July 2018; Accepted 13 August 2018; Published 2 September 2018

Academic Editor: Keigo Watanabe

A Stewart parallel robot (SPR) is a promising choice for alignment or assembly of components that are large or heavy. This paper presents a method for human-robot collaboration, for positioning and orientation of large components. Use of interactive force measurements is important for human-robot collaboration. It is based on six-dimensional force/torque (F/T) measurements. First, the six-dimensional F/T data are calculated based on the six-actuator SPR geometry and screw theory. Second, the effects of gravity forces (dynamic gravity compensation) are considered, and a method to offset their effects is explained. Third, force estimation experiments were performed using an S-type force sensor and known applied test forces. Finally, the F/T-driven feedback was tested for the alignment of a large-scale component. The experimental results show that the calculated six-dimensional F/T can accurately track the force applied to a large and/or heavy component by a human worker. It can also accurately predict the F/T required to compensate for inertial forces and components' weight. Thus, the alignment method of human-robot collaboration based on the six-dimensional force/torque dynamic measurements for large-scale components is correct and effective.

1. Introduction

With the constant increase in the difficulty of assembly and the numbers of large-scale satellite cabins, rocket cabins, ship cabins, and other large and/or heavy assemblies, the assembly requirements for large-size and heavy-weight components present obstacles. These can include safety risks for workers. Currently, assembly methods based on manual operations have many problems such as physical difficulty for workers, high collision risks, inadequate precision, and low productivity.

Modern industrial practice is moving towards intelligence, diversification, and personalization. Human-robot collaborations have become hot spots in the field of robotics. Such robots allow people to enter their work spaces and collaborate to complete operations. Robots and humans no longer need to work separately. This type of collaborative process not only takes advantage of the large load capacity, high stability, and high-precision position and orientation (P&O) capabilities of robots but also complements the capabilities of people for on-site observation and task flexibility [1, 2]. The team of Mitsantisuk introduced a new force sensor less haptic human-robot collaboration system based on 3D parallel mechanism delta robot, and the controller of delta robot was designed with considering of gravity compensation [3]. The team of Geravand introduced two examples of reaction schemes for collaboration, with the user pushing/pulling the robot at any point of its structure (e.g., for manual guidance) or with a compliant-like robot behaviour in response to forces applied by the human [4].

An industrial robot's characteristics of high load capacity, high-precision P&O control, and good stability mean it can offer stable and accurate positioning of heavy components. In recent years, parallel robots have been widely used for P&O of the large components and assemblies, due to these advantages as well as high stiffness and rapid motion [5, 6]. Stewart parallel robots (SPRs) are the most frequently used type of parallel robot structure. They are suitable for

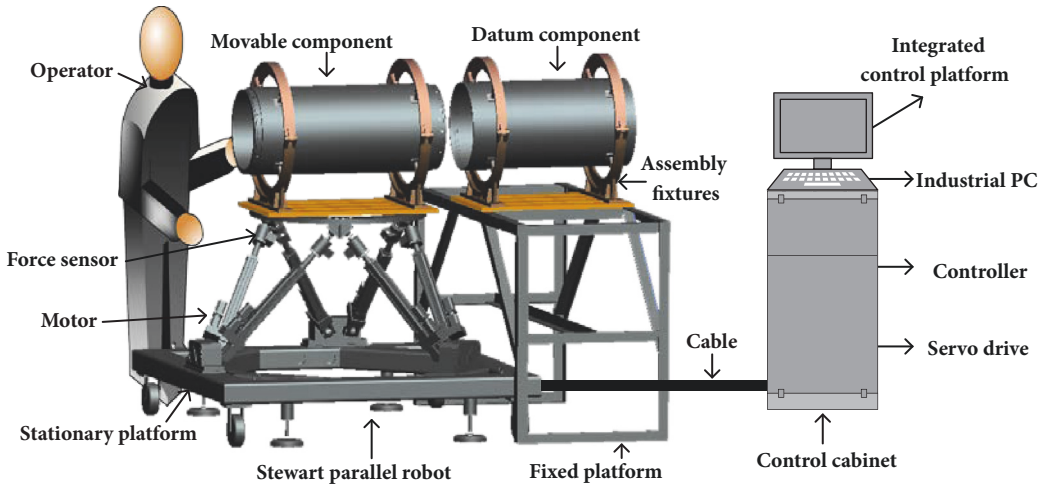

FIGURE 1: The large-scale alignment system with an SPR for large components.

machining and manufacturing [7, 8], surgical operations [9], flight simulators [10], flexible and precise assembly of aircraft sections [11], P&O of spacecraft on the ground [12], and low-impact alignments [13]. An SPR is composed of a moving platform and a base platform, which are connected by six extensible links with spherical/universal joints. In its operational range, 6-Degrees-of-Freedom (DOF) motion of the moving platform can be achieved by the motions of the six limbs as a group [14, 15]. The SPR's limbs' position and their force measurements are also very important [16]. In 2016, the team of Du from Beihang University presented an analytical algorithm of six-dimensional F/T by measuring limbs' position and their force based on a SPR [17]. It laid the foundation for the research of this paper.

In the process of human-robot collaboration, methods of compensating for the weight of an unknown load are a research hot spot. In general, the mass and center of gravity of the load are not known in advance, so it is necessary to estimate them online. In 2015, the team of Liu from South China University of Technology analyzed the center of gravity of the load according to the relationship between force and torque and then used this calculation to compensate for the effect of load center of gravity on the required screw torque [18]. In 2016, Mitsantisuk of Thai Agricultural University proposed a solution for human-robot collaboration using a delta parallel robot. A disturbance observer was used at the drive joint of the delta robot, to assist in judging the load characteristics by observing additional torque at each drive joint beyond the torque required for motion of the unloaded robot. They also compensated for gravity [3]. In 2017, Boisclair of Laval University in Canada studied a method combining of gravity compensation and the six-dimensional force/torque (F/T) sensor with a cylindrical Halbach array. The cylindrical Halbach array was installed at the joint of an industrial robot and generated joint torque through a magnetic field to compensate the additional torque of the load precisely [19]. In 2017, using six-dimensional F/T sensors and a set of calibration and calculation methods, the team of Zhang from Beijing Institute of Spacecraft Environment Engineering eliminated the effect of sensor zero and load gravity on force perception and accurately obtained the external force and torque applied at the load end of the robot [20, 21].

As mentioned above, human-robot collaboration is becoming more and more important in the assembly of large and heavy components, and SPR's are widely used in this type of process. In this paper, an SPR design is described which can adjust the P&O of the component and dynamically measure interactive forces. Then, the dynamic gravity deviations are considered and accurately compensated for. Lastly, the large-scale alignment experiments were carried out, using an SPR incorporating the six-dimensional F/T dynamic measurements.

2. Large-Scale Alignment System Using an SPR and a Human

The large-scale alignment system with a Stewart parallel robot (SPR) for large components is shown in Figure 1. It includes an SPR, fixed platform, control cabinet, assembly fixtures, movable component, datum component, and an operator. The SPR is designed based on a 6-SPS (six limbs, each with an actuator, spherical hinge-prismatic pair-spherical hinge) Stewart parallel robot and six force sensors, which can adjust the P&O of the moving platform and dynamically measure six-dimensional F/T from the interactive force. It contains a moving platform, stationary platform (base platform), force sensors, AC servo motors, and branched chains. One of the SPR's six force sensors is placed in each limb to measure the limbs' actuation force to calculate the six-dimensional F/T data.

The principles for positioning and aligning components are described in this paper. They are based on the measured six-dimensional F/T data and the input forces from a human operator on a component. These principles are shown by the flowchart in Figure 2.

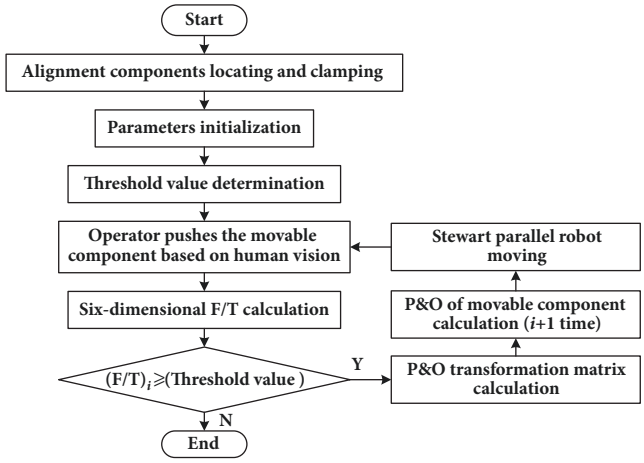

Figure 2: The human-SPR component alignment flowchart based on the measured six-dimensional F/T data.

3. Six-Dimensional Force/Torque Dynamic Measurement of the SPR

3.1. Method of Measuring Six-Dimensional F/T Based on the SPR. As presented in Figure 3, the SPR consists of a moving platform and a stationary platform, which are connected to each other with six limbs, adjustable in length through sliding joints. In the operation range, the 6-DOF motion of the moving platform could be achieved by the motions of the six limbs. Force sensors are placed in each limb to measure the limbs' actuation force f_i. Encoders are used to measure the limbs' length l_i ($i = 1, \ldots, 6$). The Cartesian coordinate system of o_0-$x_0y_0z_0$ is located in the center of the top surface of the base platform, while the Cartesian coordinate system of o_1-$x_1y_1z_1$ is located in the center of the bottom surface of the moving platform. The centers of the spherical joints are denoted as A_i and B_i. $[\boldsymbol{F}_s\ \boldsymbol{M}_s]^T$=$[F_x,F_y,F_z,M_x,M_y,M_z]^{\mathrm{T}}$ is expressed the external load which is decomposed in o_1-$x_1y_1z_1$. $\boldsymbol{A}_i$ is the coordinate in o_1-$x_1y_1z_1$. $\boldsymbol{B}'_{\boldsymbol{i}}$ is the coordinate in o_1-$x_1y_1z_1$ and $\boldsymbol{B}_i$ is the coordinate in o_0-$x_0y_0z_0$. The two vectors are different descriptions of the same point; hence they can be related using a linear transformation as follows:

$$B'_i = R_{3\times3}{}^{-1} \cdot \left(\left(B_i\right)_{3\times1} - M_{3\times1}\right) \tag{1}$$

where $\boldsymbol{R}_{\boldsymbol{3\times3}}$ represents a rotation matrix and $\boldsymbol{M}_{\boldsymbol{3\times3}}$ represents a translation matrix. Once the distance between A_i and B_i (limb length l_i) is set, the P&O parameters $\{x\ y\ z\ \alpha\ \beta\ \gamma\}$ between o_1-$x_1y_1z_1$ and o_0-$x_0y_0z_0$ could be solved by the newton iteration method. Among the P&O parameters, $\{x\ y\ z\}$ is the position vector of o_1-$x_1y_1z_1$, with respect to o_0-$x_0y_0z_0$, and $\{\alpha\ \beta\ \gamma\}$ is the orientation angle of o_1-$x_1y_1z_1$, with respect to o_0-$x_0y_0z_0$. Thus, $\boldsymbol{R}_{\boldsymbol{3\times3}}$ and $\boldsymbol{M}_{\boldsymbol{3\times3}}$ can be expressed as

$$R = \begin{bmatrix} \cos\alpha\cos\beta & \cos\alpha\sin\beta\sin\gamma - \sin\alpha\cos\gamma & \cos\alpha\sin\beta\cos\gamma + \sin\alpha\sin\gamma \\ \sin\alpha\cos\beta & \sin\alpha\sin\beta\sin\gamma + \cos\alpha\cos\beta & \sin\alpha\sin\beta\cos\gamma - \cos\alpha\sin\gamma \\ -\sin\beta & \cos\beta\sin\gamma & \cos\beta\cos\gamma \end{bmatrix} \tag{2}$$

$$M = \begin{bmatrix} x & y & z \end{bmatrix}^T \tag{3}$$

The force equilibrium equation could be defined in the o_1-$x_1y_1z_1$ using the screw theory as

$$F_s + \in M_s = \sum_{i=1}^{6} f_i \$_i \tag{4}$$

where $\$_{\boldsymbol{i}}$ is the unit screw along the i^{th} leg and could be obtained by $\$_{\boldsymbol{i}} = [\boldsymbol{S}_{\boldsymbol{i}}, \boldsymbol{S}_{\boldsymbol{0i}}]^{\boldsymbol{T}}$. $\boldsymbol{S}_i$ is the unit vector of f_i with respect to o_1-$x_1y_1z_1$. $\boldsymbol{S}_{0i}$ is the torque vector of $\boldsymbol{S}_i$ with respect to o_1-$x_1y_1z_1$. According to (1), $\boldsymbol{S}_i$ and $\boldsymbol{S}_{0i}$ could be calculated as

$$S_i = \frac{A_i - B_i}{\left\|A_i - B_i\right\|}$$
$$S_{0i} = A_i \times S_i \tag{5}$$

Equation (4) can be rewritten in the form of matrix equation as

$$F = [G]\, f \tag{6}$$

where

$$F = \begin{bmatrix} F_s & M_s \end{bmatrix}^T = \begin{bmatrix} F_x & F_y & F_z & M_x & M_y & M_z \end{bmatrix}^T \tag{7}$$

$$f = \begin{bmatrix} f_1 & f_2 & f_3 & f_4 & f_5 & f_6 \end{bmatrix}^T \tag{8}$$

$$[\boldsymbol{G}] = \begin{bmatrix} \boldsymbol{S}_1 & \boldsymbol{S}_2 & \boldsymbol{S}_3 & \boldsymbol{S}_4 & \boldsymbol{S}_5 & \boldsymbol{S}_6 \\ \boldsymbol{S}_{01} & \boldsymbol{S}_{02} & \boldsymbol{S}_{03} & \boldsymbol{S}_{04} & \boldsymbol{S}_{05} & \boldsymbol{S}_{06} \end{bmatrix} \tag{9}$$

Hence, the external load $[\boldsymbol{F}_s\ \boldsymbol{M}_s]^T$ can be calculated by (6).

3.2. Dynamic Gravity Compensation. During the assembly process, the moving platform, assembly fixtures, and components are relatively heavy and bulky, so their barycenter and gravity deviations, which are caused by manufacturing errors and installation errors, will lead to wrong calculation results of the six-dimensional F/T. The dynamic gravity compensation is needed.

The influential factors of the calculation results, which are the barycenter and gravity of the moving platform, assembly fixtures, and other components, cannot be ignored. This

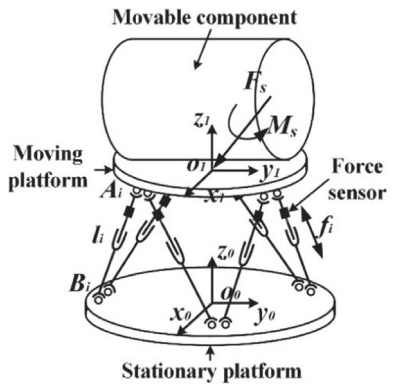

Figure 3: The theoretical model for a six-dimensional F/T based on the SPR.

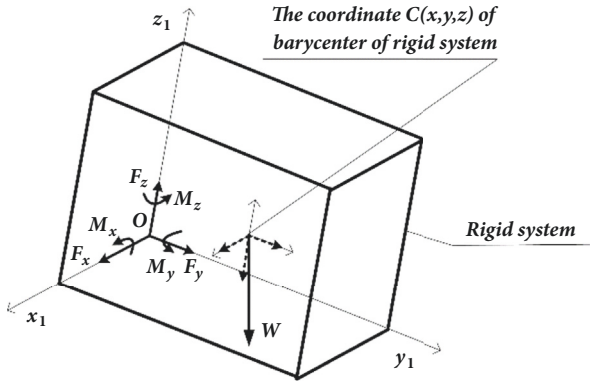

Figure 4: Schematic diagram of gravity of the rigid system in o_1-$x_1y_1z_1$.

paper considers them as a rigid system. Equation (6) can be thus rewritten as

$$F + \begin{bmatrix} S_G \\ S_{0G} \end{bmatrix} W = [G]\, f \tag{10}$$

where W is the dimensionless value of the gravity, so it is not a vector. $\boldsymbol{S}_G$ is the gravity unit vector of the said rigid system, so it is a 3-column vector. $\boldsymbol{S}_{0G}$ is the torque vector of $\boldsymbol{S}_G$ with respect to o_1-$x_1y_1z_1$, so $\boldsymbol{S}_{0G}$ is also a 3-column vector.

When the external load is zero, the six-dimensional F/T is caused by the gravity of the rigid system (as in Figure 4). The coordinate $\boldsymbol{C}=[x\ y\ z]^{\mathrm{T}}$ indicates the barycenter of the rigid system in o_1-$x_1y_1z_1$. According to the least square principle, $\boldsymbol{C}$ and W can be solved by the six-dimensional F/T under three different P&O sets. As an example, four measurements are performed here:

$$\begin{bmatrix} M_{x1} & M_{x2} & M_{x3} & M_{x4} \\ M_{y1} & M_{y2} & M_{y3} & M_{y4} \\ M_{z1} & M_{z2} & M_{z3} & M_{z4} \end{bmatrix} = \begin{bmatrix} 0 & -z & y \\ z & 0 & -x \\ -y & x & 0 \end{bmatrix} \begin{bmatrix} F_{x1} & F_{x2} & F_{x3} & F_{x4} \\ F_{y1} & F_{y2} & F_{y3} & F_{y4} \\ F_{z1} & F_{z2} & F_{z3} & F_{z4} \end{bmatrix} \tag{11}$$

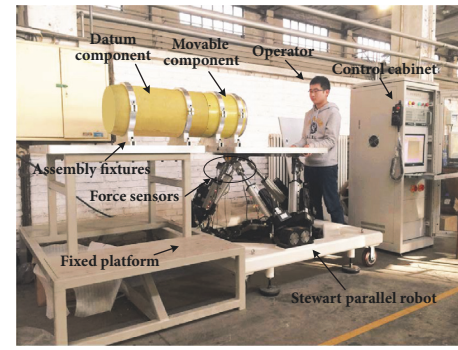

Figure 5: The large-scale alignment system with a SPR supporting a large component.

The resolving process of $\boldsymbol{C}$ and W from (11) is similar to that of the generalized inverse matrix of

$$\begin{bmatrix} F_{x1} & F_{x2} & F_{x3} & F_{x4} \\ F_{y1} & F_{y2} & F_{y3} & F_{y4} \\ F_{z1} & F_{z2} & F_{z3} & F_{z4} \end{bmatrix}. \tag{12}$$

When P&O changes, $\boldsymbol{C}$ and W of the rigid system do not differ in o_1-$x_1y_1z_1$, and the direction $\boldsymbol{S} = [0\ 0\ -1]^{\mathrm{T}}$ of gravity does not vary in o_0-$x_0y_0z_0$, meaning

$$S_G = \frac{R^{-1} \cdot S}{\left\| R^{-1} \cdot S \right\|}$$
$$S_{0G} = C \times S_G \tag{13}$$

which could serve for the solution of (10).

For the preparation of a six-dimensional F/T measurement, experiments without external loads were carried out first, and the measured F/Ts could be used for the calculations of $\boldsymbol{C}$ and W, using (11), after which $\boldsymbol{C}$ is substituted into (13) for the vector $[\boldsymbol{S}_G\ \boldsymbol{S}_{0G}]^T$. Then, for an arbitrary external load, the six-dimensional F/T in o_1-$x_1y_1z_1$ could be obtained using (10) and the gravity of the rigid system can be dynamically compensated.

4. Experimental Results and Discussion

The component alignment system using an SPR to align large components is designed as shown in Figure 5. It includes the SPR, fixed platform, control cabinet, assembly fixtures, movable component, datum component, and operator. The parameters of the SPR are listed in Table 1.

4.1. Measurement of Known Applied Force. An S-type force sensor (with an accuracy of ±0.03 N) is used to measure the magnitude of applied force in real time. The operator applies the force to the SP or component to be moved, and the force is transmitted through the SPR to the S-type force sensor. The value of the six-dimensional F/T data can then be calculated and compared with the measurement value of the S-type force sensor. Datapoints were collected every 0.05 s during the experiment. The results are presented in Figure 6.

Table 1: The parameters of the SPR.

Parameter name	Value
Moving range along x direction	±50 mm
Moving range along y direction	±50 mm
Moving range along z direction	±50 mm
Rotation range along x direction	±5°
Rotation range along y direction	±5°
Rotation range along z direction	±5°
Maximum load	800 kg
Accuracy	0.05 mm
Overall size	1.5m×1.5m×1m

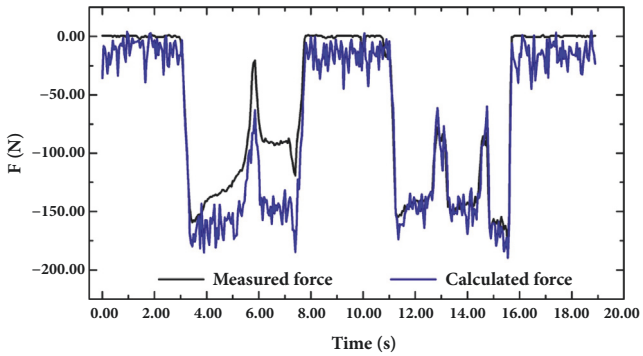

Figure 6: Comparison between the measured forces and calculated forces.

To measure an applied force, three steps were followed in this experiment. The first step is to compensate for the weight of the SPR and component, and the dynamic forces due to motion. When no external forces are applied to the SPR, any four groups of P&O parameters are selected as inputs to the SPR. Then, the four groups of the six-dimensional F/T can be calculated. The weight and center of gravity of the rigid body (moving platform, assembly fixture, and movable component) are inputs to the dynamic gravity compensation method. The weight is 1969.1017 N. The barycentric coordinate of the rigid body is $[-36.7749, -6.2296, -208.3247]^{T}$ in o_1-$x_1y_1z_1$. Second, the mean values of the six-dimensional F/T data are calculated. Due to measurement errors that caused the six-dimensional F/T data to fluctuate, the mean values of 100 groups of the six-dimensional T/F data are taken as the reference zero values. Finally, the six-dimensional F/T data are calculated. Figure 6 compares actual force data, as applied by the operator, to the input (interactive) force calculated by the system. These F/T data allows the system to estimate the interactive force between a person and the SPR or load component.

The results compared in Figure 6 show that the SPR system can accurately track the actual (measured) interactive force. The measured force and the calculated force are in good agreement, with an average error magnitude of 14.70 N (the difference between measured force and calculated force is taken as the absolute value, and then the average error magnitude is taken). Thus, these experimental results verify that this method of using six-dimensional SPR F/T data can track the operator's actual force inputs.

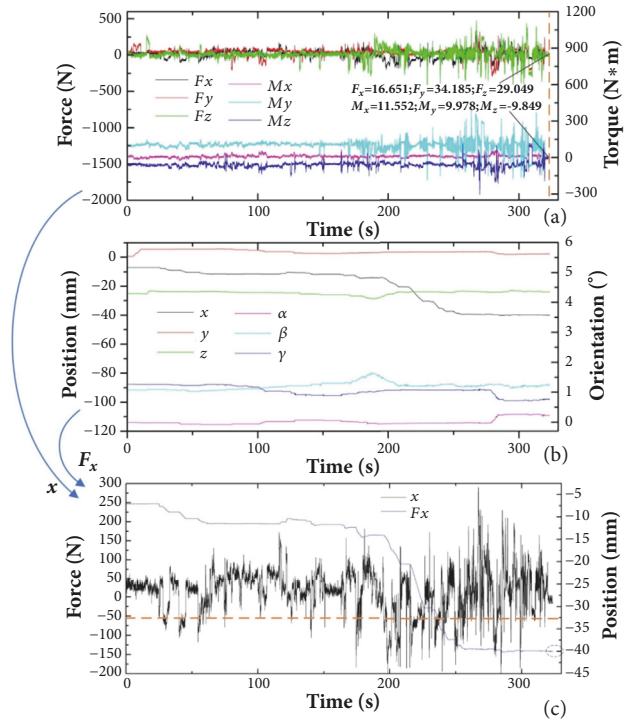

Figure 7: P&O and F/T curves over time.

4.2. F/T-Driven Alignment of Large Components. The operator applies the force to the SPR, and the SPR adjusts the P&O of large component to follow the intentions of the operator. Thus, the F/T feedback-driven alignment of large components can be implemented as in Figure 2. It is described as follows. First, some parameters are initialized, and the threshold values of six-dimensional F/T are obtained by experimental optimization. The applied threshold value of the force magnitude was 60 N, and the applied threshold value of the torque magnitude was 25 N∗m. Second, the operator visually judged the direction of the desired motion, and the external force was applied to the SPR by the operator. Third, the six-dimensional F/T tensor was calculated in real time by the dynamic force and weight compensation. This interactive force is taken as an input to the SPR. Fourth, the process of the F/T-driven alignment of large components was then executed though the direction and magnitude of interactive force and torque inputs. At last, the SPR adjusts the P&O of large component to follow the intentions of the operator. The experiment and the result are presented in Figure 7.

In Figure 7(a), when the calculated force $|F_x|$ is greater than the threshold value 60N, the SPR moved along the -x directions, until it stops at about -40 mm. At this location, the alignment process was successfully completed. Small changes in other degrees of freedom indicate that the components have high assembly accuracy and the adjustment range is

small aside from the -x movement (as shown in Figure 7(b)). After the alignment process is completed, the maximum force value in the six-dimensional F/T is 35 N, and the maximum torque value is 12 N∗m (as shown in Figure 7(a)). These experimental results demonstrate that the calculation method of the six-dimensional F/T based on the SPR is correct, and the F/T-driven alignment of large components is effective.

5. Conclusions

The SPR can adjust the P&O of the component and dynamically measure forces from interaction between a robot and a human. The experimental results show that the forces due to weight can be reliably compensated for. The contributions of the paper are summarized as follows:

(1) A method of measuring six-dimensional F/T, based on the SPR characteristics and screw theory, is proposed for the accurate estimation of the external forces during alignment of large-scale components. Forces due to gravity are taken into consideration, and a precise weight compensation method is provided.

(2) Known applied force measurement experiments are performed on the SPR using an S-type force sensor. The six-dimensional F/T can accurately track the change of the measurement force and the average error is about 14.70 N. The experiment of F/T-driven alignment for large component was successfully completed.

(3) Interactive force measurements are important for human-robot collaboration. The proposed method fulfills the requirement for accurate force estimation. It provides satisfactory compensation for forces due to gravity, in order to accurately separate forces due to the interaction of a human with a robot. The measurements from the six-dimensional F/T based on the SPR could be further improved with more accurate measurements of the forces and the limb lengths' variation with motion.

Data Availability

The data used to support the findings of this study are available from the corresponding author upon request.

Conflicts of Interest

The authors declare that there are no conflicts of interest regarding the publication of this paper.

Acknowledgments

This work was supported by the National Key R&D Program of China [2017YFB1301800].

References

[1] B. Yao, Z. Zhou, L. Wang, W. Xu, Q. Liu, and A. Liu, "Sensorless and adaptive admittance control of industrial robot in physical human−robot interaction," *Robotics and Computer-Integrated Manufacturing*, vol. 51, pp. 158–168, 2018.

[2] J. Krüger, T. K. Lien, and A. Verl, "Cooperation of human and machines in assembly lines," *CIRP Annals - Manufacturing Technology*, vol. 58, no. 2, pp. 628–646, 2009.

[3] C. Mitsantisuk and K. Ohishi, "Haptic human-robot collaboration system based on delta robot with gravity compensation," in *Proceedings of the 42nd Conference of the Industrial Electronics Society, IECON 2016*, pp. 5796–5801, Italy, October 2016.

[4] M. Geravand, F. Flacco, and A. De Luca, "Human-robot physical interaction and collaboration using an industrial robot with a closed control architecture," in *Proceedings of the 2013 IEEE International Conference on Robotics and Automation, ICRA 2013*, pp. 4000–4007, Germany, May 2013.

[5] A. Seibel, S. Schulz, and J. Schlattmann, "On the Direct Kinematics Problem of Parallel Mechanisms," *Journal of Robotics*, vol. 2018, Article ID 2412608, 9 pages, 2018.

[6] R. Yao, W. Zhu, and P. Huang, "Accuracy analysis of Stewart platform based on interval analysis method," *Chinese Journal of Mechanical Engineering*, vol. 26, no. 1, pp. 29–34, 2013.

[7] B. Denkena, C. Holz, and H. Abdellatif, "Model-based control of a hexapod with linear direct drives," *International Journal of Computer Integrated Manufacturing*, vol. 19, no. 5, pp. 463–472, 2006.

[8] S. Pedrammehr, M. Mahboubkhah, and N. Khani, "A study on vibration of Stewart platform-based machine tool table," *The International Journal of Advanced Manufacturing Technology*, vol. 65, no. 5–8, pp. 991–1007, 2013.

[9] M. Moradi Dalvand and B. Shirinzadeh, "Motion control analysis of a parallel robot assisted minimally invasive surgery/microsurgery system (PRAMiSS)," *Robotics and Computer-Integrated Manufacturing*, vol. 29, no. 2, pp. 318–327, 2013.

[10] A. Pisla, T. Itul, D. Pisla, and A. Szilaghyi, "Considerations upon the influence of manufacturing and assembly errors on the kinematic and dynamic behavior in a flight simulator stewart-gough platform," *Mechanisms and Machine Science*, vol. 3, pp. 215–223, 2012.

[11] C. Löchte, F. Dietrich, and A. Raatz, "A Parallel Kinematic Concept Targeting at More Accurate Assembly of Aircraft Sections," in *Intelligent Robotics and Applications*, vol. 7101 of *Lecture Notes in Computer Science*, pp. 142–151, Springer Berlin Heidelberg, Berlin, Heidelberg, 2011.

[12] Y. Xu, J. Yuan, J. Zhao, and Y. Zhao, "Robust attitude control and simulation of a Stewart spacecraft," in *Proceedings of the 2015 27th Chinese Control and Decision Conference (CCDC)*, pp. 477–482, Qingdao, China, May 2015.

[13] H. Zhao, S. Zhang Y, and D. Chen X, "Compliant force control in space docking," in *Proceedings of the 2007 IEEE International conference on mechatronics and automation*, Harbin, China, Aug, 2007.

[14] G. Zhang, J. Du, and S. To, "Calibration of a small size hexapod machine tool using coordinate measuring machine," *Proceedings of the Institution of Mechanical Engineers, Part E: Journal of Process Mechanical Engineering*, vol. 230, no. 3, pp. 183–197, 2014.

[15] W. Zhou, W. Chen, H. Liu, and X. Li, "A new forward kinematic algorithm for a general Stewart platform," *Mechanism and Machine Theory*, vol. 87, pp. 177–190, 2015.

[16] S. A. Maged, A. M. R. Fath El Bab, and A. A. Abouelsoud, "An adaptive observer for a Stewart platform manipulator using leg position and force measurements," *International Journal of Modelling, Identification and Control*, vol. 24, no. 1, pp. 62–74, 2015.

[17] K. Wen, F. Du, and X. Zhang, "Algorithm and experiments of six-dimensional force/torque dynamic measurements based on a Stewart platform," *Chinese Journal of Aeronautics*, vol. 29, no. 6, pp. 1840–1851, 2016.

[18] B. Liu W, *Research on Industrial Robot Grinding based on Force Control*, South China University of Technology, 2014.

[19] J. Boisclair, P.-L. Richard, T. Laliberté, and C. Gosselin, "Gravity Compensation of Robotic Manipulators Using Cylindrical Halbach Arrays," *IEEE/ASME Transactions on Mechatronics*, vol. 22, no. 1, pp. 457–464, 2017.

[20] L.-J. Zhang, R.-Q. Hu, and W.-M. Yi, "Research on Force Sensing for the End-load of Industrial Robot Based on a 6-axis Force/Torque Sensor," *Zidonghua Xuebao/Acta Automatica Sinica*, vol. 43, no. 3, pp. 439–447, 2017.

[21] L. Zhang J, R. Hu Q, and W. Yi M, "A Study of Flexible Force Control Method on Robotic Assembly for Spacecraft," *Applied Mechanics Materials*, vol. 681, pp. 79–85, 2014.